Predictions of decay modes for the superheavy nuclei most suitable for synthesis *

Jun-Hong Liu(刘俊宏)[1] Shu-Qing Guo(郭树青)[1] Xiao-Jun Bao(包小军)[2] Hong-Fei Zhang(张鸿飞)[1;1)]

[1] School of Nuclear Science and Technology, Lanzhou University, Lanzhou 730000, China
[2] College of Physics and Information Science, Hunan Normal University, Changsha 410006, China

Abstract: The competition between α-decay and spontaneous fission of superheavy nuclei (SHN) is investigated by the generalized liquid drop model (GLDM) and the modified Swiatecki's formula respectively. The theoretical decay modes are in good agreement with the experimental results. Predictions are made for as-yet unobserved superheavy nuclei. The theoretical calculations show that the nuclei $^{298}120$, $^{295}119$, $^{290}118$, $^{291}117$, $^{287}117$, $^{294}116$, $^{289}116$, $^{286}116$, $^{285}116$, $^{284}115$, $^{283}115$, $^{283}114$, $^{282}114$, $^{280}113$, $^{276}112$, $^{275}112$, $^{274}112$, $^{273}111$, $^{272}110$, $^{265}109$ may be synthesized experimentally in the near future since they not only have relatively large predicted cross sections but can also be identified via α-decay chains.

Keywords: superheavy nuclei, α-decay, spontaneous fission

PACS: 21.10.Tg, 23.60.+e, 27.90.+b **DOI:** 10.1088/1674-1137/41/7/074106

1 Introduction

α-decay and spontaneous fission (SF) are the dominant decay modes for the superheavy nuclei (SHN), and they can be taken as the limiting factor that determines the stability of SHN. Great success has been achieved during the last two decades in the experimental study of reactions leading to SHN. Up to now, the synthesis of SHN (Z=107–112) has been achieved by cold fusion of heavy ions with Pb or Bi as targets [1–3]. Hot fusion reactions with ^{48}Ca as projectiles have also been applied to synthesize the elements Z=112–118 [4–6]. The most significant outcome of these recent measurements is the observed increase in half-lives with increasing neutron number, which is consistent with the predicted increased stability of SHN when approaching $N = 184$. However, the unambiguous identification of the new isotopes still poses a problem because their α-decay chains are terminated by SF before reaching the known region of the nuclear chart. The understanding of the competition between α-decay and spontaneous fission channels in SHN is of crucial importance for our ability to map the SHN region and to assess its extent [7–12].

The newly synthesized elements or new isotopes are mainly identified by decay chains from unknown nuclei to known nuclei with the help of the parent-daughter correlation. The competition between fission and α-decay plays a crucial role in the detection of these superheavy nuclei in the laboratory. In fact, α-decay is not only a very powerful tool to investigate the nuclear structure properties of unstable nuclei, but also a reliable way to identify the newly synthesized superheavy elements [13–19]. Many theoretical efforts have been devoted to pursuing a quantitative description of α-decay phenomena. These studies are based on various theoretical models such as the shell model, fission-like model, cluster model, and so on [20–29]. Spontaneous fission is also one of the most important decay modes for heavy and superheavy nuclei with proton number $Z \geqslant 90$. Recently, the spontaneous fission half-lives of several SHN have been measured by different laboratories. According to the classical liquid drop model, all superheavy nuclei should be unstable against spontaneous fission due to the strong Coulomb repulsion. However, although the fission barrier disappears in SHN in the liquid drop model, the nuclear shell effect leads to a relatively high fission barrier and eventually stabilizes SHN [30–32]. The physical mechanism of the spontaneous fission is rather complex and there are large uncertainties in the fission process, such as the treatment of the multidimensional deformations, and the corresponding nuclear structure-dependent tensor of mass inertia. Thus a full microscopic treatment of such a multidimensional system is extremely difficult. Moreover, the multidimensional

Received 5 March 2017

∗ Supported by National Natural Science Foundation of China (11675066) and Feitian Scholar Project of Gansu Province

1) E-mail: zhanghongfei@lzu.edu.cn

potential energy surface alone is not sufficient for accurate determination of the corresponding half-life. So the most realistic calculations of the spontaneous fission half-lives are based on the the search for the least action path in the multidimensional deformation space [33–35]. In addition, a detailed knowledge of the mass inertia parameters is required. Furthermore, the analysis can be performed only in a rather restricted area of the nuclear deformation map due to long calculation times. Another method applied for the calculation of the spontaneous fission half-lives is the phenomenological approach. Several authors have proposed an empirical formula for determining the half-lives of spontaneous fission. A systematic study of the relation between Z and A and half-lives should make it possible to come to a better understanding of this process. Seaborg [36] and Whitehouse [37] plotted the logarithm of the spontaneous fission half-lives of several nuclides as a function of the parameter Z^2/A, and observed that the logarithm of the spontaneous fission half-lives of even-even nuclides decreases with Z^2/A values in a linear manner. A deviation from the above correlation is discussed in Ref. [38]. It is shown that the spontaneous fission half-lives of the even-even isotopes go through a maximum with increasing A for fixed Z number. Moreover, Swiatecki [39] discussed the regular dependence of the half-life on ground-state masses, which plays an important role for establishing a physical interpretation. Swiatecki proposed a semi-empirical formula for spontaneous fission half-lives of even-even, odd A and odd-odd nuclei. By using this formula the author successfully reproduced the experimental data. Recently, we generalized Swiatecki's formula with a set of new parameters for spontaneous fission half-lives, and the experimental half-lives are reproduced well for heavy and superheavy nuclei [40].

In the present work, we systematically study the competition between α-decay and SF in the superheavy region and investigate the properties of some unknown SHN, such as $^{290}118$, $^{295}119$ and $^{298}120$, which are most likely to be synthesized in upcoming experiments owing to the relatively large predicted evaporation residual cross sections [41, 42]. Although these candidate unknown SHN may have a great chance of being synthesized, whether or not they can be detected in the experiments depends on the following conditions: (1) whether the half-lives of these nuclei are large enough (larger than about 1 μs) to allow for their observation; (2) whether the main decay mode of the SHN is α-decay and if so (3) whether the unknown SHN could link to the known nuclei via α-decay chains. In fact, all of the above conditions should be checked theoretically before preparing for the corresponding experiments. In the present work, all these arguments will be discussed. The main goal is to predict the decay modes for new isotopes which may possibly be synthesized in upcoming experiments.

2 Theoretical methods

2.1 α-decay

2.1.1 GLDM

In the framework of the generalized liquid drop model (GLDM) [43], the alpha decay is governed by the potential energy including the volume, surface, Coulomb and proximity energies:

$$E_{\rm GLDM}=E_{\rm V}+E_{\rm S}+E_{\rm C}+E_{\rm prox}. \tag{1}$$

For a one-body configuration, the volume energy $E_{\rm V}$, surface energy $E_{\rm S}$ and Coulomb energy $E_{\rm C}$ are defined as:

$$E_{\rm V}=-a_{\rm V}(1-\kappa_{\rm V}I^2)A, \tag{2}$$

$$E_{\rm S}=a_{\rm S}(1-\kappa_{\rm S}I^2)A^{2/3}\frac{S}{4\pi R_0^2}, \tag{3}$$

$$E_{\rm C}=0.6e^2\frac{Z^2}{R_0}\frac{1}{2}\int\frac{V(\theta)}{V_0}\left(\frac{R(\theta)}{R_0}\right)^3\sin\theta{\rm d}\theta, \tag{4}$$

where A, Z and $I=(N-Z)/A$ are the mass number, charge number and relative neutron excess, respectively. $V(\theta)$ is the electrostatic potential at the surface and V_0 is the surface potential of the sphere. The volume and surface coefficient are $a_{\rm V}=15.494$ MeV and $a_{\rm S}=17.9439$ MeV, respectively. The volume and surface asymmetric coefficient are $\kappa_{\rm V}=1.8$ and $\kappa_{\rm S}=2.6$, respectively. The effective radii R_0 are given by

$$R_0=(1.28A^{1/3}-0.76+0.8A^{-1/3})\ {\rm fm}. \tag{5}$$

Owing to the effects of the nuclear forces between close surfaces, the proximity energy $E_{\rm prox}$ must be taken into account.

$$E_{\rm prox}=2\gamma\int_{h_{\rm min}}^{h_{\rm max}}\phi\left[\frac{D(r,h)}{b}\right]2\pi h{\rm d}h, \tag{6}$$

where h is the distance varying from the neck radius or zero to the height of the neck border. D is the distance between the surfaces and $b=0.99$ fm is the surface width. ϕ is the Feldmeier proximity function. The surface parameter γ is the geometric mean between the surface parameters of the two fragment nuclei.

$$\gamma=0.9517\sqrt{(1-k_{\rm S}I_1^2)(1-k_{\rm S}I_2^2)}{\rm MeV/fm^2}. \tag{7}$$

After the two bodies are separated, the volume energy $E_{\rm V}$, surface energy $E_{\rm S}$ and Coulomb energy $E_{\rm C}$ are:

$$E_{\rm V}=-a_{\rm V}[(1-k_{\rm V}I_1^2)A_1+(1-k_{\rm V}I_2^2)A_2], \tag{8}$$

$$E_{\rm S}=a_{\rm S}[(1-k_{\rm S}I_1^2)A_1^{\frac{2}{3}}+(1-k_{\rm S}I_2^2)A_2^{\frac{2}{3}}], \tag{9}$$

$$E_{\rm C}=\frac{0.6e^2Z_1^2}{R_1}+\frac{0.6e^2Z_2^2}{R_2}+\frac{e^2Z_1Z_2}{r}, \tag{10}$$

where A_i, Z_i, R_i and I_i are the masses, charges, radii and relative neutron excesses of the two fragments, respectively.

The α-decay half-life is calculated using the WKB barrier penetration probability, with the decay constant λ and half-life $T_{1/2}$ of the α emitters defined as:

$$\lambda=P_\alpha\nu_0 P, \tag{11}$$

$$T_{1/2}=\frac{\ln 2}{\lambda}, \tag{12}$$

where ν_0 is the assault frequency. For α-decay, the ν_0 has been taken as: $\nu_0=\frac{1}{2R}\sqrt{\frac{2E_\alpha}{M_\alpha}}$. R is the radius of the parent nucleus, E_α is the kinetic energy of the emitted α particle and M_α is the mass of the α particle. P_α is the preformation factor. The corresponding details of P_α are presented in a previous study [44]. The barrier penetrability P is calculated with the action integral:

$$P=\exp\left[-\frac{2}{\hbar}\int_{R_{\rm in}}^{R_{\rm out}}\sqrt{2B(r)[E(r)-E(\text{sphere})]}\mathrm{d}r\right]. \tag{13}$$

2.1.2 The Viola-Seaborg semiempirical relationship

The Viola-Seaborg formula with Sobiczewski constants is given as [45, 46]

$$\log_{10}[T_{1/2}(\text{s})]=(aZ+b)Q^{-1/2}+cZ+d+h_{\log}. \tag{14}$$

The constants are $a=1.66175$, $b=-0.85166$, $c=-0.20228$, $d=-33.9069$, and $h_{\log}=0$ for Z, N even nuclei, $h_{\log}=0.772$ for Z=odd, N=even nuclei, $h_{\log}=1.066$ for Z=even, N=odd nuclei, $h_{\log}=1.114$ for Z, N odd nuclei.

2.1.3 The Royer analytical formula

The Royer formula is quite an accurate expression for α-decay proposed in 2000 [47]. The subset of the 131 even-even nuclei is obtained with a root mean square (RMS) deviation of only 0.285,

$$\log_{10}[T_{1/2}(\text{s})]=-25.31-1.169A^{1/6}\sqrt{Z}+\frac{1.5864Z}{\sqrt{Q_\alpha}}, \tag{15}$$

where A and Z represent the mass and charge numbers of the parent nuclei and Q_α represents the energy released during the reaction. For the subset of 106 even-odd nuclei the RMS deviation is 0.39,

$$\log_{10}[T_{1/2}(\text{s})]=-26.65-1.0859A^{1/6}\sqrt{Z}+\frac{1.5848Z}{\sqrt{Q_\alpha}}. \tag{16}$$

For the subset of the 86 odd-even nuclei and a RMS deviation of 0.36,

$$\log_{10}[T_{1/2}(\text{s})]=-25.68-1.1423A^{1/6}\sqrt{Z}+\frac{1.592Z}{\sqrt{Q_\alpha}}. \tag{17}$$

For the subset of the 50 odd-odd nuclei the following formula leads to a RMS of 0.35,

$$\log_{10}[T_{1/2}(\text{s})]=-29.48-1.113A^{1/6}\sqrt{Z}+\frac{1.6971Z}{\sqrt{Q_\alpha}}. \tag{18}$$

2.2 Spontaneous fission

The half-lives of SF can be calculated by the modified Swiatecki's formula [40]. The modified Swiatecki's formula can be written as

$$\log_{10}[T_{1/2}(\text{a})]=c_1+c_2\left[\frac{Z^2}{(1-kI^2)A}\right]+c_3\left[\frac{Z^2}{(1-kI^2)A}\right]^2+c_4E_{\rm sh}+h_{\rm i}. \tag{19}$$

The parameters in the modified formula are: $c_1=1174.353441$, $c_2=-47.666855$, $c_3=0.471307$, $c_4=3.378848$. The fixed value of k is 2.6. $h_{\rm i}$ is the blocking effect of unpaired nucleons. $h_{\rm i}=0$ for even-even nuclei, $h_{\rm i}=2.609374$ for odd-N nuclei, $h_{\rm i}=2.619768$ for the odd-Z nuclei, and $h_{\rm i}=5.22914$ for odd-odd nuclei.

3 Results and discussion

The half-lives of α-decay are calculated by the GLDM [48], the Royer formula [47] and the Viola-Seaborg semiempirical relationship (VSS) [45, 46], respectively. These models can reproduce the experimental T_α very well for heavy and superheavy nuclei when the experimental Q_α are taken. In the present work, the Q_α are extracted from the new mass table WS4 [49], which is one of the most accurate models to reproduce the experimental Q_α of SHN [50]. Calculations of half-lives of SF are employed by the modified Swiatecki's formula, with the shell correction from the FRDM1995 [51].

Table 1 shows the comparison between the experimental decay modes and the theoretical results. The first column denotes nuclei. The experimental and theoretical Q_α are shown in columns 2 and 3. Column 3 and column 4 show the experimental half-lives of SF and α-decay respectively. Column 5 shows the theoretical half-lives of SF calculated by the modified Swiatecki' s formula. Columns 6, 7 and 8 show the theoretical half-lives of α-decay calculated by the Royer analytical formula, the VSS and the GLDM respectively. The experimental decay modes and the theoretical decay modes are shown in the last two columns [52]. As shown in Table 1, all the three different models can reproduce the experimental α-decay half-lives well, and the modified Swiatecki's formula can also reasonably reproduce the SF half-lives. Some predictions of SF half-lives of the SHN with no experimental measurements have been made. The decay mode is determined by the channel with the most probability (short life-time). The calculated decay modes are in good agreement with the experimental result. To some extent, the result of calculated SF half-lives is reasonable.

Figure 1 shows the results of the calculated decay modes in the superheavy region. On one hand, our calculated decay modes can reproduce the fact that α-decay mainly occurs at the region of neutron deficiency as shown in Fig. 1 by yellow squares. On the other hand,

Table 1. Comparison between the predicted decay modes and the experimental decay modes.

nuclei	$Q_\alpha^{\rm exp.}$ [52]	$Q_\alpha^{\rm th.}$	$T_{1/2}^{\rm SF}$/s(exp.) [52]	$T_{1/2}^{\alpha}$/s(exp.) [52]	$T_{1/2}^{\rm SF}$/s(th.)	$T_{1/2}^{\alpha}$/s(Royer)	$T_{1/2}^{\alpha}$/s(VSS)	$T_{1/2}^{\alpha}$/s(GLDM)	mode(exp.)	mode(th.)
^{294}118	11.82	12.17	—	6.90×10^{-04}	$4.63\times10^{+04}$	5.93×10^{-05}	9.75×10^{-05}	1.31×10^{-04}	α	α
^{294}117	11.18	11.35	—	5.10×10^{-02}	$4.46\times10^{+11}$	2.59×10^{-02}	5.28×10^{-02}	3.41×10^{-03}	α	α
^{293}117	11.32	11.60	—	2.20×10^{-02}	$1.90\times10^{+08}$	1.51×10^{-03}	6.24×10^{-03}	3.16×10^{-03}	α	α
^{293}116	10.71	10.77	—	5.70×10^{-02}	$1.06\times10^{+09}$	1.71×10^{-01}	7.00×10^{-01}	1.30×10^{-01}	α	α
^{292}116	10.78	11.10	—	1.30×10^{-02}	$2.20\times10^{+05}$	4.61×10^{-03}	8.51×10^{-03}	6.97×10^{-03}	α	α
^{291}116	10.89	11.09	—	1.90×10^{-02}	$1.53\times10^{+07}$	2.75×10^{-02}	1.03×10^{-01}	2.61×10^{-02}	α	α
^{290}116	11.00	11.06	—	8.30×10^{-03}	$5.14\times10^{+03}$	6.47×10^{-03}	1.10×10^{-02}	1.11×10^{-02}	α	α
^{290}115	10.41	10.26	—	6.50×10^{-01}	$8.02\times10^{+10}$	$5.68\times10^{+00}$	$9.08\times10^{+00}$	8.63×10^{-01}	α	α
^{289}115	10.49	10.27	—	3.30×10^{-01}	$1.31\times10^{+07}$	9.12×10^{-01}	$3.85\times10^{+00}$	$1.89\times10^{+00}$	α	α
^{288}115	10.63	10.37	—	1.64×10^{-01}	$5.01\times10^{+09}$	$2.88\times10^{+00}$	$4.46\times10^{+00}$	3.80×10^{-01}	α	α
^{287}115	10.76	10.47	—	3.70×10^{-02}	$5.61\times10^{+05}$	2.74×10^{-01}	$1.07\times10^{+00}$	6.66×10^{-01}	α	α
^{289}114	9.98	9.58	—	$1.90\times10^{+00}$	$3.59\times10^{+07}$	$8.17\times10^{+01}$	$3.60\times10^{+02}$	$7.25\times10^{+01}$	α	α
^{288}114	10.07	9.62	—	6.60×10^{-01}	$1.05\times10^{+03}$	$1.25\times10^{+01}$	$2.35\times10^{+01}$	$1.74\times10^{+01}$	α	α
^{287}114	10.17	9.74	—	4.80×10^{-01}	$2.69\times10^{+05}$	$2.86\times10^{+01}$	$1.16\times10^{+02}$	$2.97\times10^{+01}$	α	α
^{286}114	10.35	9.94	3.00×10^{-01}	2.00×10^{-01}	$3.46\times10^{+01}$	$1.52\times10^{+00}$	$2.62\times10^{+00}$	$2.39\times10^{+00}$	α/SF	α/SF
^{285}114	—	10.25	—	1.30×10^{-01}	$2.09\times10^{+04}$	$1.10\times10^{+00}$	$4.10\times10^{+00}$	$1.31\times10^{+00}$	α	α
^{286}113	9.79	9.46	—	$9.50\times10^{+00}$	$9.33\times10^{+06}$	$3.08\times10^{+02}$	$4.17\times10^{+02}$	$6.09\times10^{+01}$	α	α
^{285}113	10.01	9.78	—	$4.20\times10^{+00}$	$1.10\times10^{+03}$	$4.88\times10^{+00}$	$2.10\times10^{+01}$	$1.03\times10^{+01}$	α	α
^{284}113	10.12	10.09	—	9.10×10^{-01}	$3.27\times10^{+05}$	$3.75\times10^{+00}$	$6.27\times10^{+00}$	7.85×10^{-01}	α	α
^{283}113	10.38	10.38	—	7.50×10^{-02}	$3.85\times10^{+01}$	1.13×10^{-01}	4.55×10^{-01}	2.71×10^{-01}	α	α
^{282}113	10.78	10.87	—	7.30×10^{-02}	$9.08\times10^{+03}$	2.42×10^{-02}	5.20×10^{-02}	5.64×10^{-03}	α	α
^{285}112	9.32	9.21	—	$2.80\times10^{+01}$	$6.41\times10^{+01}$	$2.32\times10^{+02}$	$1.08\times10^{+03}$	$2.11\times10^{+02}$	α	α/SF
^{284}112	—	9.52	9.80×10^{-02}	—	7.00×10^{-03}	$5.36\times10^{+00}$	$1.01\times10^{+01}$	$6.21\times10^{+00}$	SF	SF
^{283}112	9.66	9.82	$\geq4.20\times10^{+01}$	$4.20\times10^{+00}$	$2.07\times10^{+00}$	$3.61\times10^{+00}$	$1.55\times10^{+01}$	$3.65\times10^{+00}$	α/SF	α/SF
^{282}112	——	10.11	9.10×10^{-04}	—	1.65×10^{-04}	1.12×10^{-01}	1.94×10^{-01}	1.41×10^{-01}	SF	SF
^{281}112	10.46	10.46	—	1.00×10^{-01}	2.41×10^{-02}	6.81×10^{-02}	2.69×10^{-01}	8.08×10^{-02}	α	α/SF

from the systematic distribution of the decay modes of SHN, shell corrections of SHN in the region of deformed and spherical neutron magic number ($160<N<164$ for $104<Z<110$ and $176<N<184$, for $115<Z<120$) increase the SF half-lives faster than α-decay half-lives, leading the nuclei in that regions α-decay dominated. Furthermore, our results can also reproduce the odd-even oscillation of decay modes well, taking the $Z=112$ isotopic chain for example, as seen in Fig. 1 and Table 1. The sensitive change of SF half-lives may contribute to the odd-even oscillation of decay modes, which will also be discussed in the following.

The logarithm of α-decay half-lives with the three different methods can reproduce the experimental values and the trend well, as seen in Fig. 2 and Fig. 3. Different calculations of α-decay half-lives are almost consistent with each other, indicating the predictions of α -decay are nearly model-independent and reliable. In these figures, the half-lives of α-decay of the Z=103–106 isotopes mainly increase with the increase of neutron number, while the SF half-lives mainly decrease with the increase of neutron number. The spontaneous fission half-life is smaller than the alpha-decay life-time for neutron numbers beyond $N=162$, implying that the neutron magic number $N=162$ is important for enhancing the stability of these superheavy isotopes. The principal reason for the above α-decay half-lives trend is that the Q_α decrease with the increase of neutron number, which is mainly caused by symmetry energy [53]. That is also the reason why the neutron-deficient nuclei undergo α-decay more easily. However, the principal reason for the trend of the SF half-lives is that the shell correction decreases with the increase of neutron number in this region. The deformed neutron magic number N=162 has an impact on the SF half-lives of the Z=107–110 isotopes. We can clearly see a peak around $N=162$ on the plots of SF for the Z=107–110 isotopes. However, the peaks around N=162 on the plots of α-decay of Z=107–110 isotopes are much smaller than those of SF. Therefore we can conclude that the shell structure has a greater impact on SF than on α-decay. The plots of α-decay and SF of the Z=111–114 isotopes are very close to each other over a large range, so α-decay and SF can be competitive in this region. Moreover, as the odd-even effect of SF half-lives is much more obvious than that of α -decay half-lives, as seen in Figs. 2–4, the decay modes also show the odd-even effects in this region of SHN, as shown in Table 1 and Fig. 1. However, the Z=115–120 isotopes are dominated by α emission, as shown in Figs. 3–4. Therefore, these superheavy nuclei can be identified in the laboratory by detecting the α-decay process.

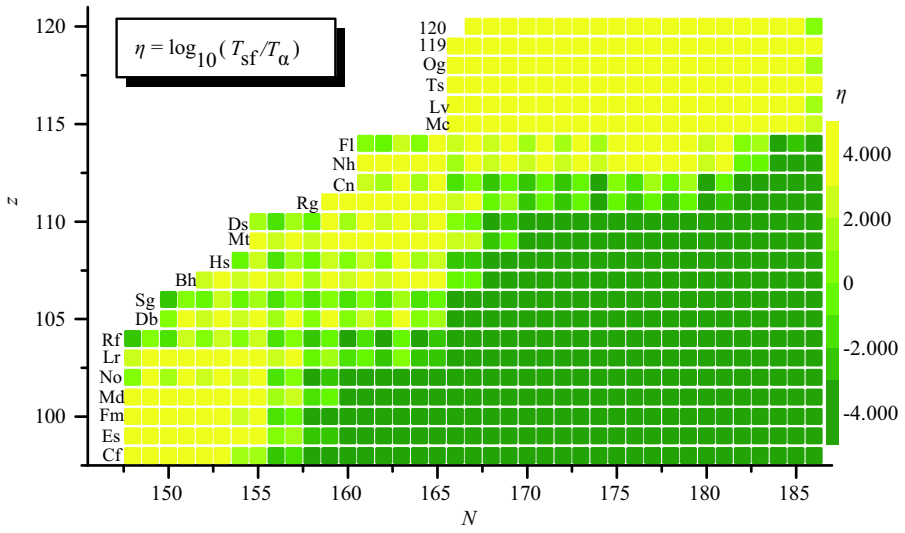

Fig. 1. (color online) Competition between α-decay and spontaneous fission.

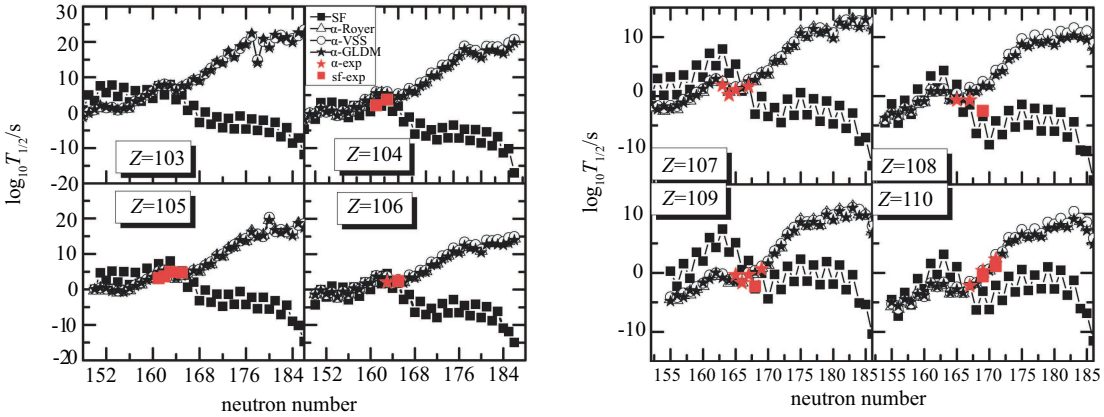

Fig. 2. (color online) Half-lives of α-decay and SF in the $103 \leqslant Z \leqslant 110$ region.

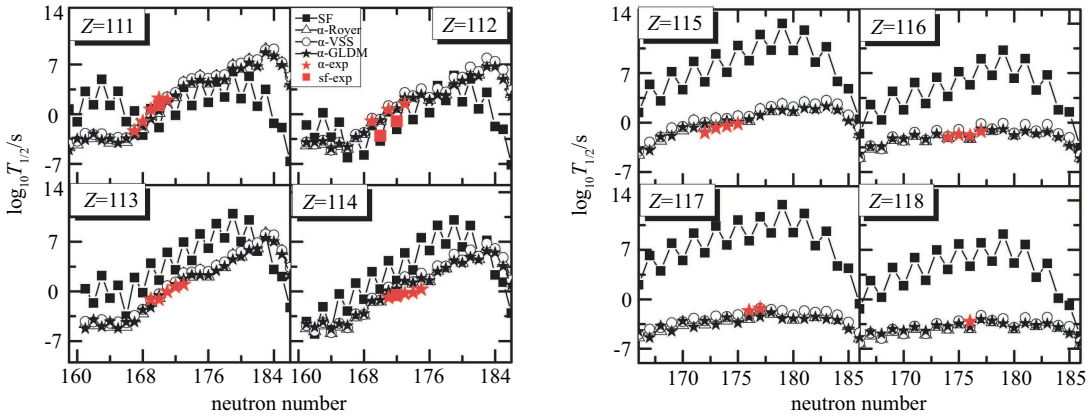

Fig. 3. (color online) Half-lives of α-decay and spontaneous fission in the $111 \leqslant Z \leqslant 118$ region.

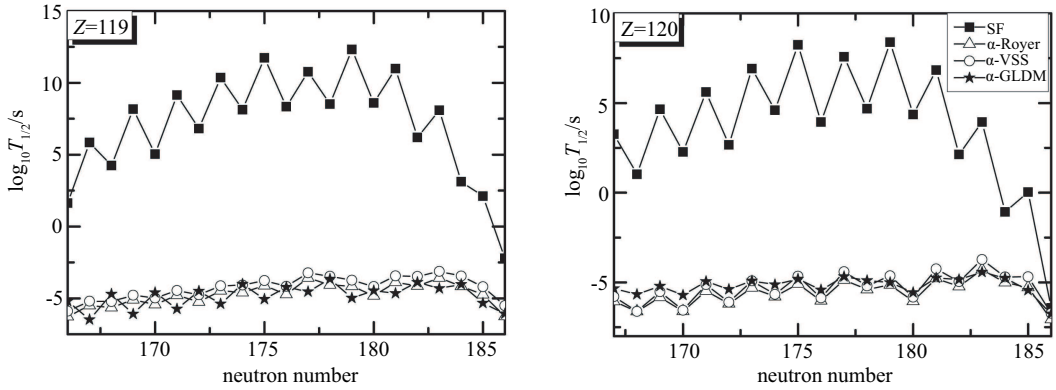

Fig. 4. Half-lives of α-decay and SF in the Z=119, 120 region.

Table 2. Decay modes of candidate nuclei.

proton number	mass number	$\log_{10}T^{\rm SF}_{1/2}$/s	$\log_{10}T^{\alpha}_{1/2}$/s(Royer)	$\log_{10}T^{\alpha}_{1/2}$/s(VSS)	$\log_{10}T^{\alpha}_{1/2}$/s(GLDM)	mode of decay
120	298	4.679	−5.396	−5.197	−4.893	α1
118	294	4.666	−4.227	−4.011	−3.882	α2
116	290	3.711	−2.189	−1.96	−1.955	α3
114	286	1.539	0.181	0.418	0.379	α4
112	282	−3.783	−0.951	−0.712	−0.852	SF
119	295	8.334	−4.735	−4.171	−4.227	α1
117	291	7.681	−3.009	−2.428	−2.574	α2
115	287	5.749	−0.563	0.028	−0.177	α3
118	290	2.698	−5.015	−4.875	−4.473	α1
116	286	1.8	−2.667	−2.513	−2.295	α2
114	282	−1.111	−3.401	−3.241	−3.114	α3
112	278	−6.142	−4.893	−4.727	−4.617	SF
117	291	7.681	−3.009	−2.428	−2.574	α1
115	287	5.749	−0.563	0.028	−0.177	α2
117	287	5.486	−3.691	−3.181	−3.079	α1
115	283	3.069	−2.576	−2.053	−2.023	α2
113	279	−3.488	−4.999	−4.454	−4.351	α3
111	275	1.25	−4.016	−3.464	−3.454	α4
109	271	4.303	−0.555	−0.013	0.007	α5
107	267	3.197	0.638	1.175	1.190	α6
116	294	6.681	−1.189	−0.884	−1.082	α1
114	290	5.756	1.436	1.748	1.530	α2
116	289	6.404	−1.658	−1.118	−1.604	α1
114	285	4.321	0.041	0.613	0.118	α2
116	286	1.8	−2.667	−2.513	−2.295	α1
114	282	−1.111	−3.401	−3.241	−3.114	α2
112	278	−6.142	−4.893	−4.727	−4.617	SF
116	285	4.404	−2.48	−2.012	−2.250	α1
114	281	1.168	−3.677	−3.181	−3.393	α2
112	277	−1.143	−4.492	−3.967	−4.192	α3

Table 3. Decay modes of candidate nuclei (continued).

proton number	mass number	$\log_{10}T^{\rm SF}_{1/2}$/s	$\log_{10}T^{\alpha}_{1/2}$/s(Royer)	$\log_{10}T^{\alpha}_{1/2}$/s(VSS)	$\log_{10}T^{\alpha}_{1/2}$/s(GLDM)	mode of decay
115	284	7.181	−0.961	−0.747	−1.893	α1
113	280	1.961	−3.846	−3.401	−4.325	α2
111	276	3.234	−3.767	−3.286	−4.079	α3
109	272	7.412	−0.479	−0.179	−0.841	α4
107	268	7.226	2.417	2.553	2.121	α5
105	264	5.945	2.79	2.927	2.651	α6
103	260	6.199	3.131	3.267	3.200	α7
115	283	3.069	−2.576	−2.053	−2.023	α1
113	279	−3.488	−4.999	−4.454	−4.351	α2
111	275	1.25	−4.016	−3.464	−3.454	α3
109	271	4.303	−0.555	−0.013	0.007	α4
107	267	3.197	0.638	1.175	1.190	α5
114	283	2.776	−1.492	−0.957	−1.360	α1
112	279	−3.254	−3.419	−2.859	−3.241	α2/SF
110	275	1.021	−2.97	−2.385	−2.813	α3
108	271	4.308	0.629	1.232	0.857	α4
114	282	−1.111	−3.401	−3.241	−3.114	α1
112	278	−6.142	−4.893	−4.727	−4.617	SF
113	280	1.961	−3.846	−3.401	−4.325	α1
111	276	3.234	−3.767	−3.286	−4.079	α2
109	272	7.412	−0.479	−0.179	−0.841	α3
107	268	7.226	2.417	2.553	2.121	α4
105	264	5.945	2.79	2.927	2.651	α5
103	260	6.199	3.131	3.267	3.200	α6
112	280	−5.754	−2.798	−2.595	−2.635	SF
112	276	−3.256	−5.216	−5.087	−4.865	α1
110	272	−0.304	−2.528	−2.401	−2.323	α2
108	268	−0.726	−1.087	−0.965	−0.913	α3/SF
112	275	0.188	−4.17	−3.681	−3.810	α1
110	271	1.568	−2.209	−1.694	−1.860	α2
112	274	−3.312	−4.326	−4.237	−3.952	α1/SF
110	270	−2.729	−4.153	−4.062	−3.826	α2
111	273	1.313	−3.407	−2.894	−2.784	α1
109	269	1.972	−2.27	−1.756	−1.658	α2
107	265	1.083	−0.794	−0.285	−0.182	α3
110	272	−0.304	−2.528	−2.401	−2.323	α1
108	268	−0.726	−1.087	−0.965	−0.913	α2/SF
110	268	−5.434	−5.317	−5.262	−4.893	α1/SF
108	264	−4.605	−3.439	−3.389	−3.174	α2/SF
109	265	−2.297	−4.654	−4.202	−3.833	α1
107	261	0.125	−2.558	−2.114	−1.778	α2

Table 4. Synthesis and identification details of candidate nuclei.

parent nuclei	reaction channel	mode of synthesis	ERCS(pb) [41, 42]	linked nuclei
$^{298}120$	^{50}Ti+^{251}Cf	hot fusion	0.023	$^{294}118$
$^{295}119$	^{50}Ti+^{248}Bk	hot fusion	0.09	$^{287}115$
$^{290}118$	^{50}Ti+^{243}Cm	hot fusion	4.91	----
$^{291}117$	^{48}Ca+^{247}Bk	hot fusion	1.05	$^{287}115$
$^{287}117$	^{50}Ti+^{241}Am	hot fusion	3.66	$^{267}107$
$^{294}116$	^{48}Ca+^{250}Cm	hot fusion	3.63	$^{290}114$
$^{289}116$	^{50}Ti+^{243}Pu	hot fusion	4.68	$^{285}114$
$^{286}116$	^{50}Ti+^{239}Pu	hot fusion	1.79	----
$^{285}116$	^{50}Ti+^{238}Pu	hot fusion	1.08	$^{277}112$
$^{284}115$	^{50}Ti+^{237}Np	hot fusion	5.11	$^{260}103$
$^{283}115$	^{50}Ti+^{236}Np	hot fusion	5.55	$^{267}107$
$^{283}114$	^{48}Ca+^{238}Pu	hot fusion	2.12	$^{271}108$
$^{282}114$	^{50}Ti+^{235}U	hot fusion	1.59	----
$^{280}113$	^{48}Ca+^{235}Np	hot fusion	6.45	$^{260}103$
$^{276}112$	^{70}Zn+^{207}Pb	cold fusion	0.54	$^{268}108$
$^{275}112$	^{68}Zn+^{208}Pb	cold fusion	0.68	$^{271}110$
$^{273}111$	^{65}Ni+^{209}Bi	cold fusion	3.66	$^{265}107$
$^{272}110$	^{65}Ni+^{208}Pb	cold fusion	12.5	$^{268}108$
$^{265}109$	^{57}Fe+^{209}Bi	cold fusion	0.76	$^{261}107$

The nuclei $^{298}120$, $^{295}119$, $^{290}118$, $^{291}117$, $^{287}117$, $^{294}116$, $^{289}116$, $^{286}116$, $^{285}116$, $^{284}115$, $^{283}115$, $^{283}114$, $^{282}114$, $^{280}113$, $^{280}112$, $^{276}112$, $^{275}112$, $^{274}112$, $^{273}111$, $^{272}110$, $^{268}110$, and $^{265}109$ have been selected as candidate nuclei for synthesis in upcoming experiments since they have relatively large predicted cross sections [41, 42]. The decay properties of these superheavy nuclei are predicted in Table 2 and Table 3. For example, $^{290}118$ may be produced by the reaction ^{50}Ti+^{243}Cm, with the evaporation residue cross section (ERCS) being about 4.91 pb. Therefore, in the present work we calculated the half-lives of these nuclei and their decay products. Although the different models give different theoretical SF half-lives, the prediction of decay modes for these nuclei seems self-consistent. For example, the theoretical SF half-life of $^{290}118$ calculated by Smolanczuk is 0.048 s [34]. The calculation of Ren and Xu is 3.4×10^{17}s [54]. The calculation of Xu is 1.8×10^{10} s [55]. The calculation of Warda and Egido is 1.9×10^{6} s [56]. The calculation of Staszczak et al. is 0.063 s [10]. The calculation of Santhosh and Nithya is 3.0×10^{9} s [57], and our results is 499 s. However the α-decay half-live of $^{290}118$ calculated using the GLDM, Royer and VSS models are 3.4×10^{-5} s, 9.66×10^{-6} s and 1.3×10^{-5} s respectively. It is clear that the decay mode of $^{290}118$ is α-decay within all variants considered.

One can find easily from Table2 and Table3, for all variants considered, that the half-lives of these candidate nuclei are large enough (larger than about 1 μs) to allow for their observation.

For analysis of the α-decay chains in Table 2 and Table 3 in detail, we can see that 4 α-decay chains can be observed from $^{298}120$, which can link to a known nucleus ($^{294}118$). The $^{295}119$ can link to $^{287}115$ via 2 α-decay chains. 3 α-decay chains can be observed from $^{290}118$. However, $^{290}118$ cannot link with a known region because of the short spontaneous fission half-lives of $^{278}112$ terminating the α-chain towards the known nuclei. The $^{291}117$ can link with $^{287}115$ via 1 α-decay. The $^{287}117$ can link with $^{267}107$ via 5 α-decay chains. The $^{294}116$ can link with $^{290}114$ via 1 α-decay. The $^{289}116$ can link with $^{285}114$ via 1 α-decay. 2 α-decay chains can be observed from $^{286}116$. However, $^{286}116$ cannot link with the known region either. $^{285}116$ can link with $^{277}112$ via 2 α-decay chains. $^{284}115$ can link with $^{260}103$ via 6 α-decay chains. $^{283}115$ can link with $^{267}107$ via 4 α-decay chains. $^{283}114$ can link with $^{271}108$ via 3 α-decay chains. α-decay can be observed from $^{282}114$, but $^{282}114$ cannot decay to the known region. $^{280}113$ can link with $^{260}103$ via 5 α-decay chains. $^{280}112$ will not survive SF. $^{276}112$ can link with $^{268}108$ via 2 α-decay chains. $^{275}112$ can link with $^{271}110$ via α-decay. $^{274}112$ can also link with $^{270}110$ via α-decay. $^{273}111$ can link with $^{265}107$ via 2 α-decay chains. $^{272}110$ can link with $^{268}108$ via α-decay. The $^{268}110$ may not survive SF. $^{265}109$ can link with $^{261}107$ via by α-decay.

Combined with our previous work, we give the details of synthesis and identification of these candidate nuclei in a unified form in Table 4 and Fig. 4. The first column shows candidate nuclei. The reaction channel and synthesis modes are shown in the second and third columns. The evaporation residue cross sections are shown in the fourth column. The linked nuclei are shown in the fifth column. These theoretical predictions are useful to estimate the decay modes of the newly synthesized superheavy elements before they are produced experimentally.

This will be helpful for synthesis and identification of SHN in future experiments.

4 Summary

The experimental decay modes and half-lives of recently synthesized SHN have been successfully reproduced by comparing the theoretical α-decay and spontaneous fission half-lives, and predictions of the decay modes for unknown superheavy nuclei have been made. The decay properties of candidate nuclei for synthesis have been systematically investigated. The following conclusions may be drawn from the work:

(1) Within all theoretical calculations considered, the half-lives of these candidate nuclei are large enough (larger than about 1 μs) to allow for their observation.

(2) Most of these candidate nuclei can be linked with the known region with α-decay chains.

(3)The nuclei ^{298}120, ^{295}119, ^{290}118, ^{291}117, ^{287}117, ^{294}116, ^{289}116, ^{286}116, ^{285}116, ^{284}115, ^{283}115, ^{283}114, ^{282}114, ^{280}113, ^{276}112, ^{275}112, ^{274}112, ^{273}111, ^{272}110, ^{265}109 may be synthesized in experiments in the near future, since they not only have relatively large predicted cross sections but can also be identified via α-decay chains.

References

1 S. Hofmann and G. Munzenberg, Rev. Mod. Phys., **72**: 733 (2000)
2 S. Hofmann, Radiochim. Acta., **99**: 405 (2011)
3 K. Morita et al, J. Phys. Soc. Jpn., **76**: 045001 (2007)
4 Yu. Ts. Oganessian et al, Phys. Rev. C, **70**: 064609 (2004)
5 Yu. Ts. Oganessian et al, Phys. Rev. C, **74**: 044602 (2006)
6 Yu. Ts. Oganessian et al, Phys. Rev. Lett., **104**: 142502 (2010)
7 A. Baran, Z. Lojewski, K. Sieja and M. Kowal, Phys. Rev. C, **72**: 044310 (2005)
8 D. N. Poenaru, R. A. Gherghescu and W. Greiner, J. Phys. G, **40**: 105105 (2013)
9 Y. Qian and Z. Ren, Phys. Rev. C, **90**: 064308 (2014)
10 A. Staszczak, A. Baran and W. Nazarewicz, Phys. Rev. C, **87**: 024320 (2013)
11 K.P. Santhosh and B. Priyanka, Phys. Rev. C, **87**: 064611 (2013)
12 K. P. Santhosh and B. Priyanka, Phys. Rev. C, **89**: 064604 (2014)
13 P. Möller and J. R. Nix, Nucl. Phys. A, **549**: 84 (1992)
14 P. R. Chowdhury, D. N. Basu and C. Samanta, Phys. Rev. C, **75**: 047306 (2007)
15 D. S. Delion, R. J. Liotta and R. Wyss, Phys. Rev. C, **76**: 044301 (2007)
16 V. Y. Denisov and A. A. Khudenko, Phys. Rev. C, **81**: 034613 (2010)
17 A. I. Budaca and I. Silisteanu, Phys. Rev. C, **88**: 044618 (2013)
18 Y. Qian, Z. Ren and D. Ni, Phys. Rev. C, **89**: 024318 (2014)
19 P. Jachimowicz, M. Kowal and J. Skalski, Phys. Rev. C, **89**: 024304 (2014)
20 K. Varga, R. G. Lovas and R. J. Liotta, Phys. Rev. Lett., **69**: 37 (1992)
21 B. Buck, A. C. Merchant and S. M. Perez, Phys. Rev. C, **51**: 559 (1995)
22 G. Royer, Nucl. Phys. A, **848**: 279 (2010)
23 P. Mohr, Phys. Rev. C, **73**: 031301 (2006)
24 C. Xu and Z. Ren, Phys. Rev. C, **74**: 014304 (2006)
25 D. N. Poenaru, I. H. Plonski and W. Greiner, Phys. Rev. C, **74**: 014312 (2006)
26 C. Qi, F. R. Xu, R. J. Liotta and R. Wyss, Phys. Rev. Lett., **103**: 072501 (2009)
27 H. F. Zhang and G. Royer, Phys. Rev. C, **77**: 054318 (2008)
28 D. Ni and Z. Ren, Nucl. Phys. A, **825**: 145 (2009)
29 X. Bao, H. Zhang, H. Zhang, G. Royer and J. Li, Nucl. Phys. A, **921**: 85 (2014)
30 M. Bender, W. Nazarewicz and P. G. Reinhard, Phys. Lett. B, **515**: 42 (2001)
31 A. Sobiczewski and I. Muntian, Nucl. Phys. A, **734**: 176 (2004)
32 A. Dobrowolski, K. Pomorski and J. Bartel, Phys. Rev. C, **75**: 024613 (2007)
33 R. Smolanczuk, J. Skalski and A. Sobiczewski, Phys. Rev. C, **52**: 1871 (1995)
34 R. Smolanczuk, Phys. Rev. C, **56**: 812 (1997)
35 A. Sobiczewski and K. Pomorski, Prog. Part. Nucl. Phys, **58**: 292 (2007)
36 Glenn T. Seaborg, Phys. Rev., **85**: 157 (1952)
37 W. WhiteHouse and W. Galbraith, Nature, **169**: 494 (1952)
38 J. R. Huizenga, Phys. Rev., **94**: 158 (1954)
39 W. Swiatecki, Phys. Rev., **100**: 937 (1955)
40 X. J. Bao, S. Q. Guo, H. F. Zhang, Y. Z. Xing, J. M. Dong and J. Q. Li, J. Phys. G, **42**: 085101 (2015)
41 X. J. Bao, Y. Gao, J. Q. Li and H. F. Zhang, Phys. Rev. C, **92**: 034612 (2015)
42 X. J. Bao, Y. Gao, J. Q. Li and H. F. Zhang, Phys. Rev. C, **93**: 044615 (2016)
43 G. Royer and R. A. Gherghescu, Nucl. Phys. A, **699**: 479 (2002)
44 H. F. Zhang, G. Royer, Y. J. Wang, J. M. Dong, W. Zuo and J. Q. Li, Phys. Rev. C, **80**: 057301 (2009)
45 A. Sobiczewski, Z. Patyk, and S. Cwiok, Phys. Lett. B, **224**: 1 (1989)
46 V. E. Viola, Jr. and G. T. Seaborg, J. Inorg. Nucl. Chem., **28**: 741 (1966)
47 G. Royer, J. Phys. G: Nucl. Part. Phys., **26**: 1149(2000)
48 H.F. Zhang, Y. Gao, N. Wang, J.Q. Li, E.G. Zhao and G. Royer, Phys. Rev. C, **85**: 014325 (2012).
49 N. Wang, M. Liu, X. Z. Wu, J Meng, Phys. Lett. B, **734**: 215 (2014)
50 Y. Z. Wang at al, Phys. Rev. C, **92**: 064301 (2015)
51 Möller P, Nix J, Myers W and Swiatecki W, At. Data Nucl.Data Tables, **59**: 185 (1995)
52 Yu Ts Oganessian, V K Utyonkov, Rep. Prog. Phys., **78**: 036301 (2015)
53 J. Dong, W. Zuo and W. Scheid, Phys. Rev. Lett., **107**: 012501 (2011)
54 Z. Ren and C. Xu, Nucl. Phys. A, **759**: 64 (2005)
55 C. Xu, Z. Ren and Y. Guo, Phys. Rev. C, **78**: 044329 (2008)
56 M. Warda and J. L. Egido, Phys. Rev. C, **86**: 014322 (2012)
57 K. P. Santhosh and C. Nithya, Phys. Rev. C, **94**: 054621 (2016)